Cerebral Cortex (2018), doi: 10.1093/cercor/bhy012

Supplemental Information

Preterm Birth Changes Networks of Newborn Cortical Activity

Anton Tokariev[1], Susanna Stjerna[1], Aulikki Lano[2], Marjo Metsäranta[3],

J. Matias Palva[4] and Sampsa Vanhatalo[1]

[1]Department of Clinical Neurophysiology, University of Helsinki, 00029 HUS, Helsinki, Finland

[2]Department of Child Neurology, Children's Hospital, University of Helsinki and HUH, Helsinki, Finland

[3]Department of Neonatology, Children's Hospital, University of Helsinki and HUH, Helsinki, Finland

[4]Neuroscience Center, Helsinki Institute of Life Science, University of Helsinki, Helsinki, Finland

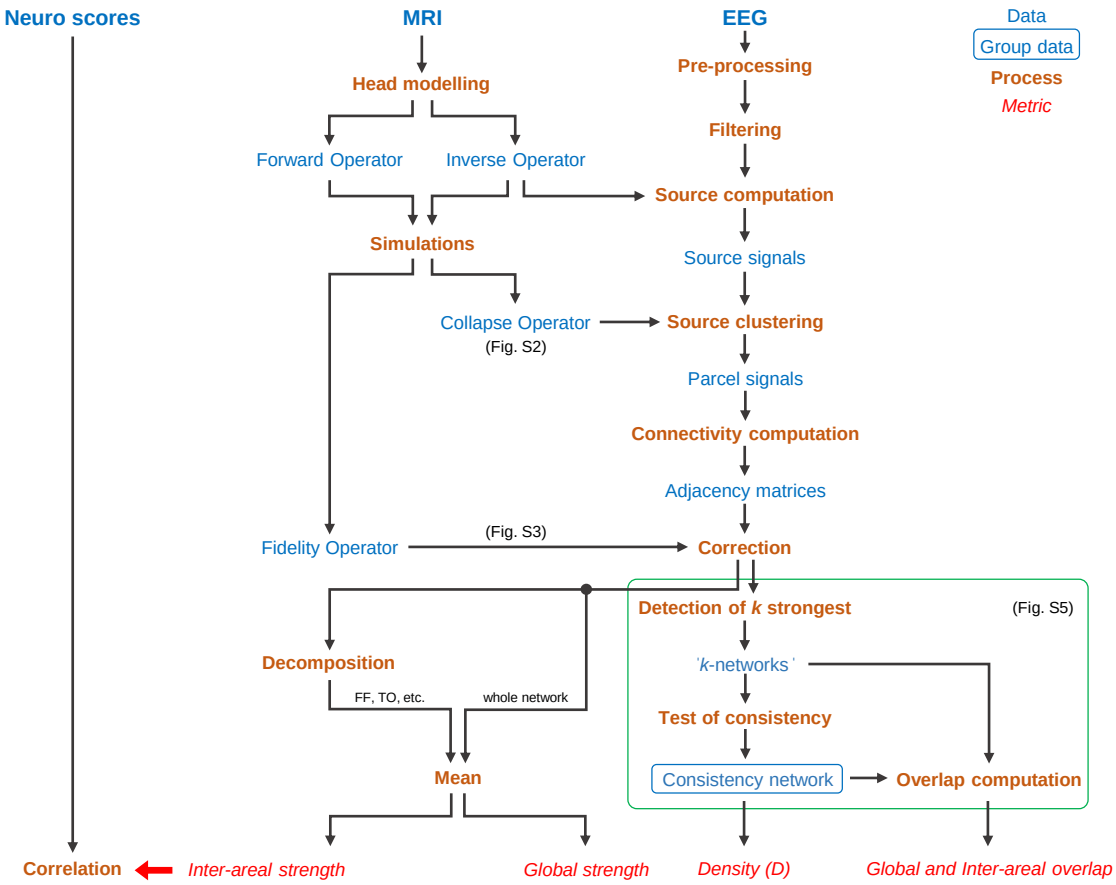

Figure S1. The overall scheme of the analysis pipeline used in this study

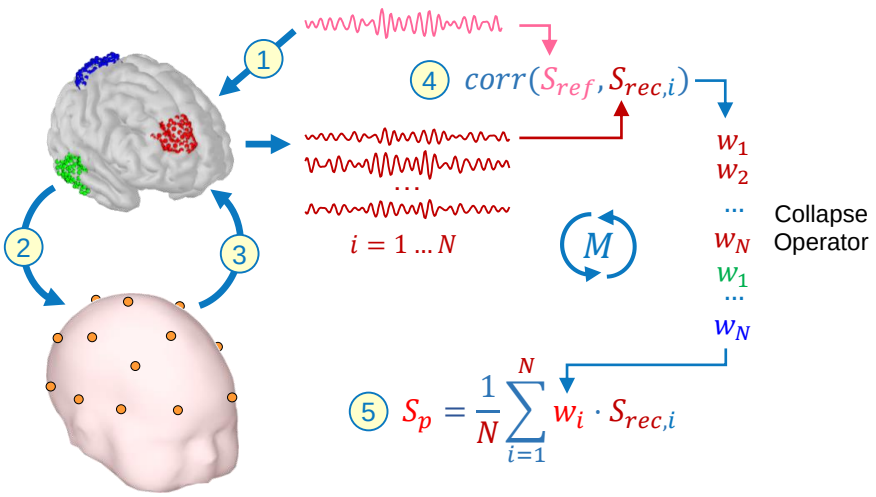

Figure S2. Computation of parcel signals. **1**, Unique simulated reference signals (S_{ref}) were assigned to each source within the same parcel. Signals were generated as a convolution of white noise with the Morlet wavelet (see **Methods** for details). Sources from all parcels were assigned own S_{ref} at the same time. **2**, EEG signals were computed from the simulated data (Forward modelling). **3**, All source signals were reconstructed back (S_{rec}) from the EEG (Inverse modelling). **4**, Weights (w) for each source within its host parcel were computed as the Pearson correlation coefficient between S_{ref} and S_{rec}. Steps **1**-**4** were repeated $M = 100$ times and median values across all iteration for the corresponding sources were used as the final weights. **5**, Parcel signal (S_p) was computed as the weighted average of all source signals within it. See also Korhonen et al. (2014).

Signal generation

Reference signals for computing *Collapse Operator* and *Fidelity Operator* were generated as a white noise $n(t)$ convoluted with the Morlet wavelet $W(t, f_0)$:

$$S_{ref}(t) = n(t) * W(t, f_0)$$

The Morlet wavelet is defined as:

$$W(t, f_0) = (\sigma_t \sqrt{\pi})^{-1/4} exp\left(\frac{-t^2}{2\sigma_t^2}\right) exp(2j\pi f_0 t)$$

It has a Gaussian shape both in the time domain with a standard deviation (SD) $\sigma_t = m/2\pi f_0$ and in the frequency domain with SD $\sigma_f = f_0/m$. Here f_0 is the nominal frequency, m is the parameter that regulates resolution between time and frequency domains, and j is an imaginary unit. We set f_0 = 10 Hz and m = 5 (see Grossmann et al., 1989). The sampling frequency of the signals was taken as *Fs* = 100 Hz and the length was 5 minutes (the same as analyzed EEG data).

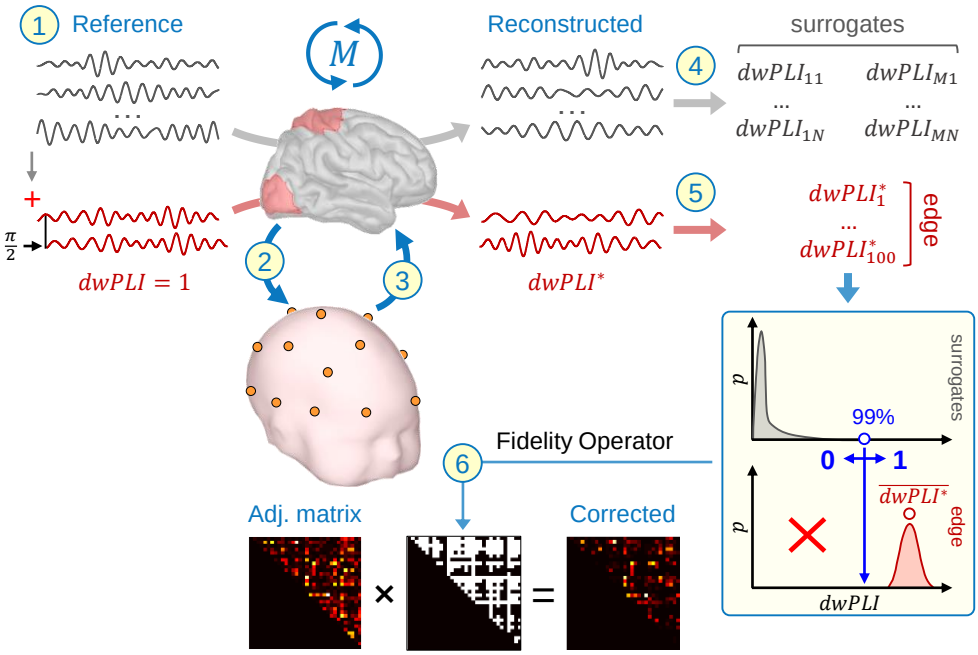

Figure S3. Adjacency matrix correction. **1**, The unique reference signals was generated for each parcel (see **Methods** for details). Surrogates (grey path) were obtained by setting all parcel signals independent, while functional coupling (red path) was simulated by setting a signal pair with phase lag $\pi/2$ (perfect synchrony; $dwPLI = 1$). **2**, Forward modelling was used to computed scalp EEG signals. **3**, Inverse modelling was used to compute source signals back with their further collapsing into parcel signals. **4**, Steps **1**-**3** were repeated $M = 500$ times to get surrogates, and for each iteration a pairwise $dwPLI$ was computed. This led to a set of about 826,500 surrogate values. **5**, For each pair of initially synchronous parcels we assessed phase synchrony between them after reconstruction ($dwPLI^*$). That was done 100 times for each edge and the mean values were taken ($\overline{dwPLI^*}$). **6**, The 99th percentile of the surrogate data was set as the threshold to define reliable edges. This led to a binary array, called ***Fidelity Operator***, where 1 stand for reliable edges and 0 – for 'rejected' ones. The correction of full adjacency matrices was done by masking it with the Fidelity Operator.

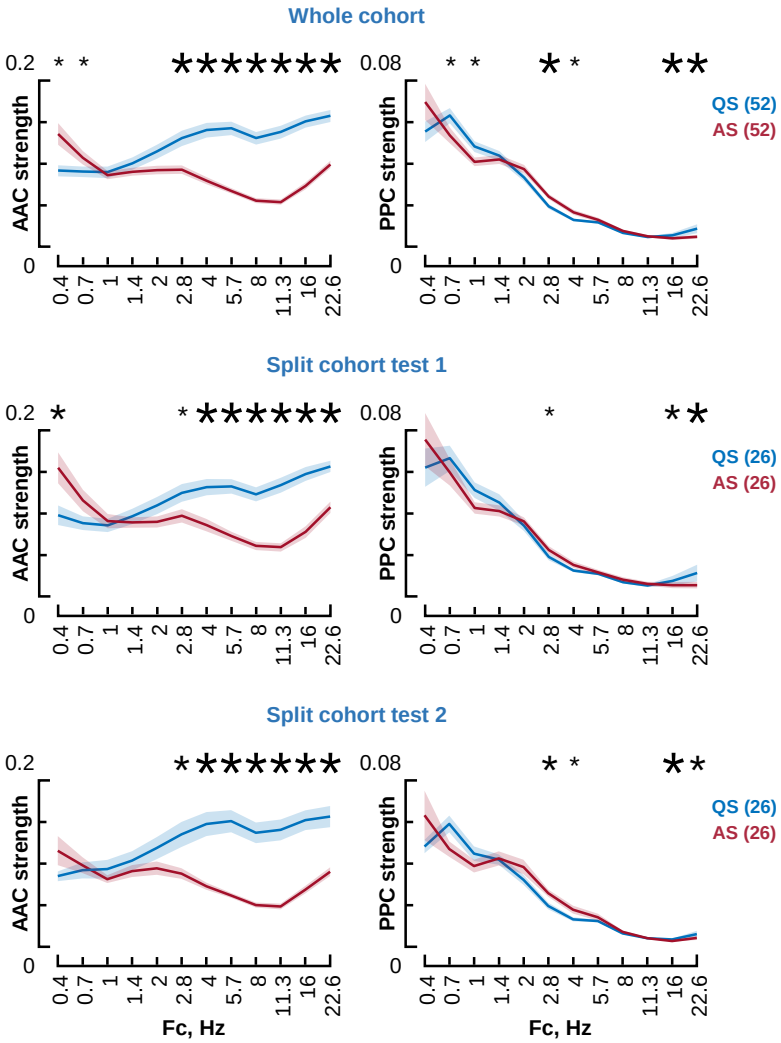

Figure S4. Split cohort test for difference in global connectivity strength between quiet sleep (QS) and active sleep (AS) in Healthy Controls. Left column refers to amplitude-amplitude correlations (AAC), right column – to phase-phase correlations (PPC). Top subplots show comparisons using the whole cohort (*N* = 52). The middle and the lower row show results obtained from the first and the second half respectively (each *N* = 26). Cohort was split according to recording date. Only subjects with both AS and QS EEG were included into the analysis. Statistical comparisons were performed using Wilcoxon sign rank test followed by post hoc correction procedure (Palva et al., 2010).

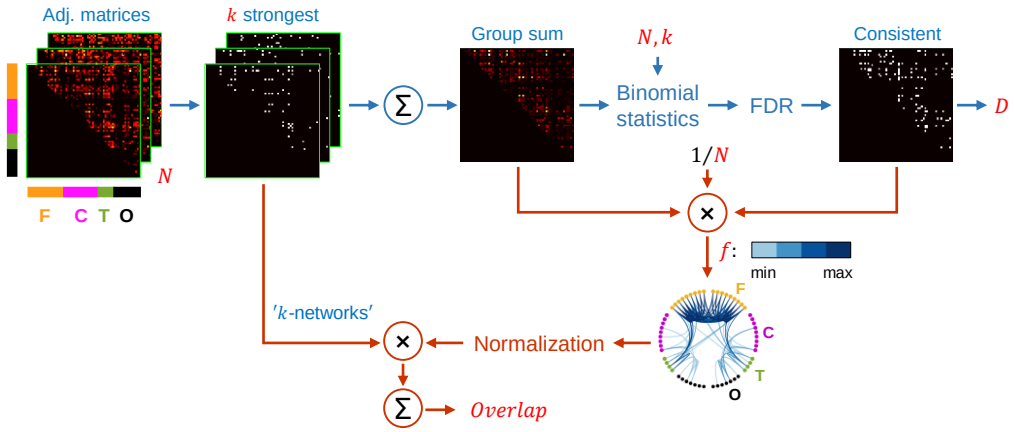

Figure S5. Computation of a consistent network, its density (blue pipeline) and overlaps of individual subsets of the strongest edges with it (red pipeline). First, *k* percent of the strongest edges is defined in each adjacency array of each subject to yield binary arrays (or 'k-networks'). The sum of these binary arrays gives a group level matrix where values in each cell indicate how many subjects in the given group present the given edge among *k*. Next, binomial statistics is used to evaluate significance of the given edge (number of trials equals the number of subjects (*N*), probability of success is set to preselected *k*, and alpha level was 0.05). The output is corrected for false discovery rate (FDR) using Benjamini-Hochberg procedure, and the result is expressed as a binary mask that depicts significant edges. This matrix is called ***consistent network*** and it represents the subset of the edges that is most frequently, or consistently, present in the given subject group. ***Density*** (*D*) is computed as a fraction of consistent network edges from the total number of edges. Frequency (*f*) of appearance for consistent edges was computed by masking the group sum matrix with the consistent network array and dividing each output element by *N*. The array containing *f* values was normalized so the sum of its elements was equal to 1 and this was used as a reference to compute overlap. Finally, ***overlap*** values were computed by multiplying individual 'k-networks' with their group reference and taking sum of the output. See also Omidvarnia et al. (2014). Matlab code that implements this algorithm is available here: https://github.com/babyEEG/neoNets.

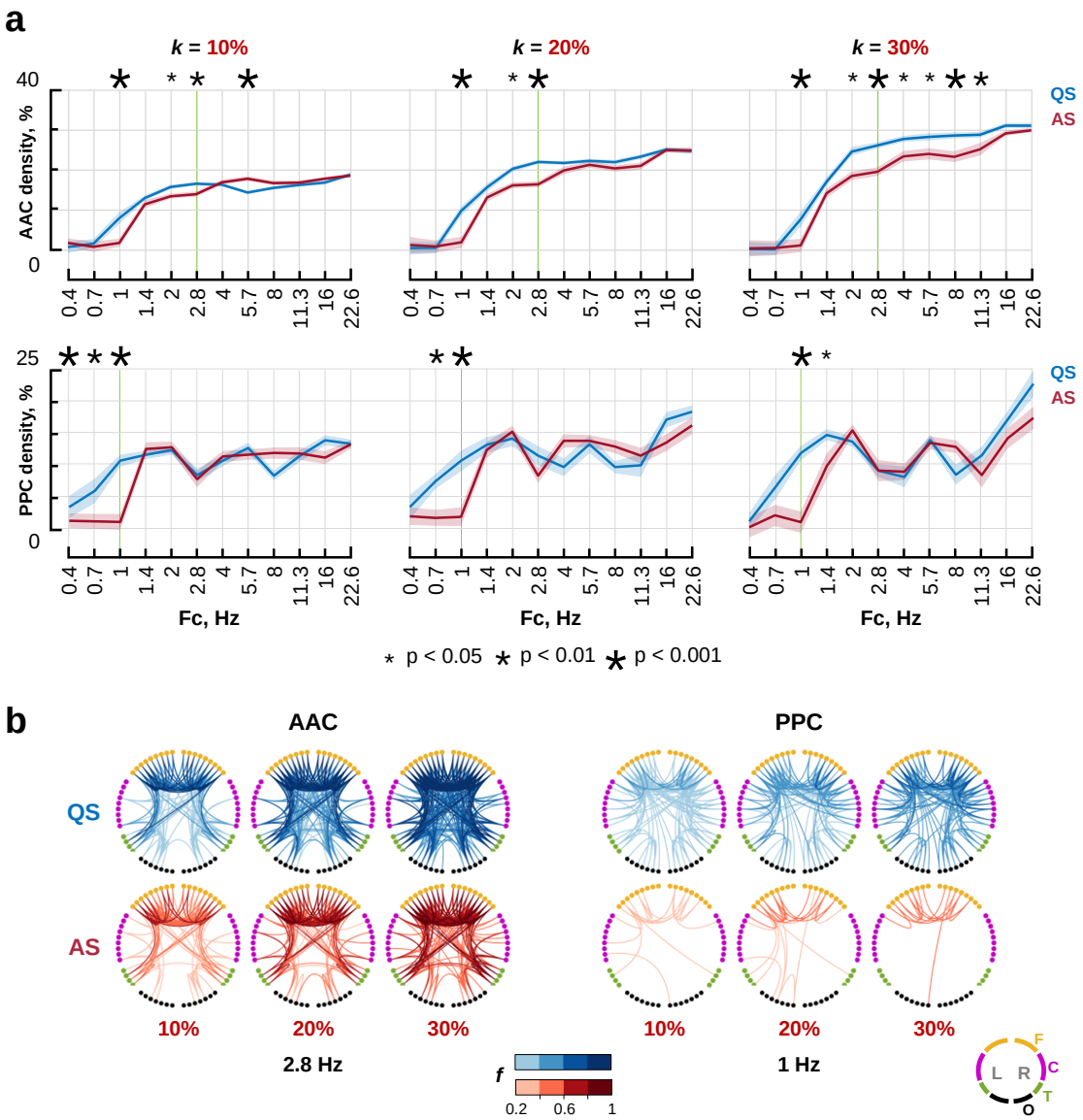

Figure S6. Effect of threshold (*k*) on the consistent networks and their comparison between quiet sleep (QS) and active sleep (AS) in Healthy Controls. **a**, We reproduced the comparisons of consistent edges densities (see **Methods** and **Supplemental** Fig. S5) using *k* = 10, 20, and 30%. The upper panel shows results for amplitude-amplitude correlation (AAC) networks, the bottom – for phase-phase correlation (PPC) networks. Statistical testing of density differences was performed using bootstrapping approach (*N* = 200 surrogates for each case). The results suggest that the differences in consistent networks densities between sleep states are robust to a range of *k* values. **b**, Examples of the spatial distributions of the consistent edges computed with different *k*. Note how the global topology remains stable despite the overall increase in the number of edges in networks as the *k* rises. Frequency of edge appearance within the subject group (*f*) is shown with different hues of color.

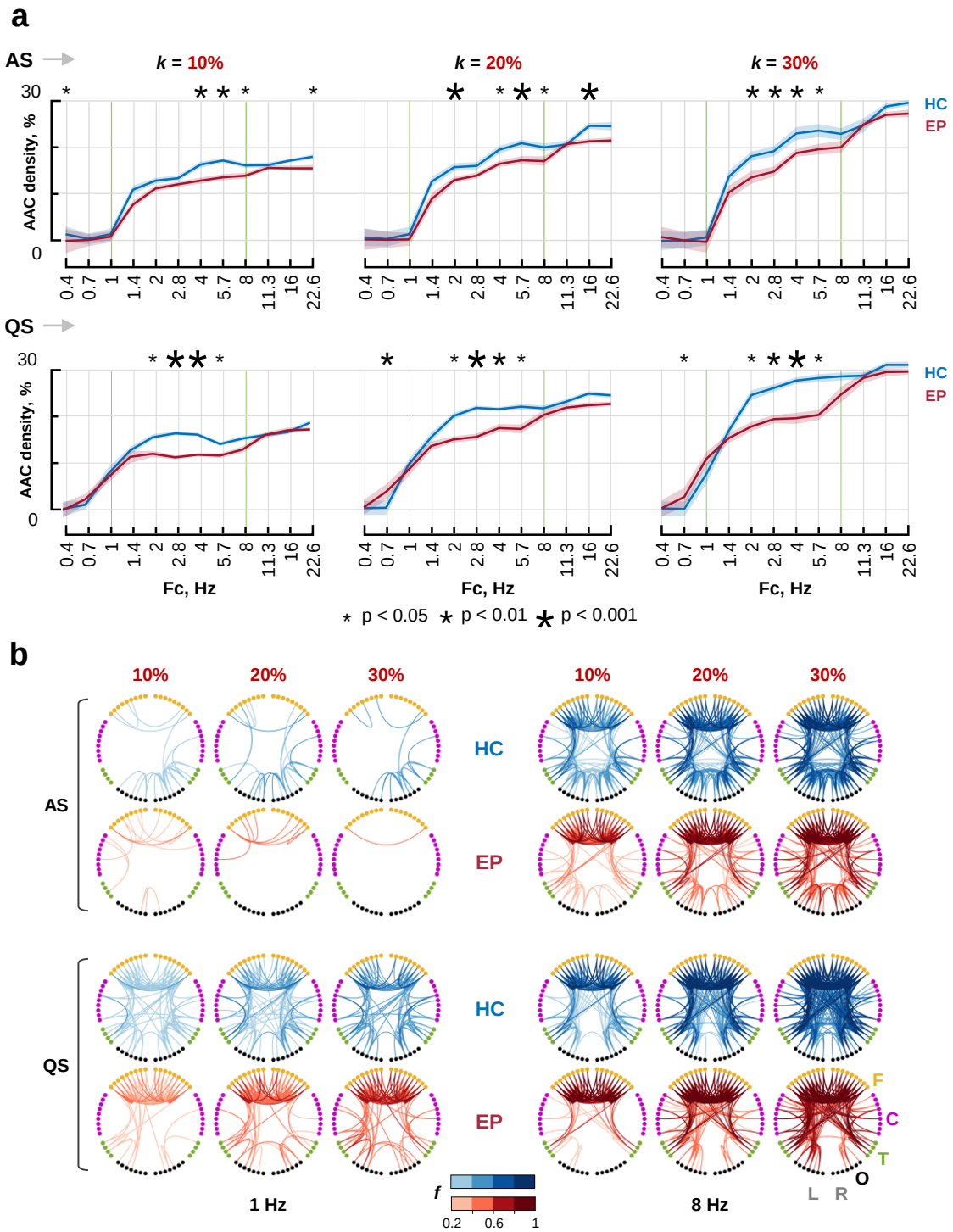

Figure S7. Effect of the threshold selection (*k*) on the consistent AAC networks and their comparison between Healthy Controls (HC) and Early Preterm (EP) infants. **a**, We reproduced the density comparisons (see **Methods** and **Supplemental** Fig. S5) using *k* = 10, 20, and 30%. The panels show results in active sleep (AS; top) and quiet sleep (QS; bottom). Statistical testing was performed using bootstrapping (*N* = 200 surrogates for each case). The results suggest that significant differences in densities between groups are robust to different *k* values. **b**, Examples of the spatial distributions of the consistent edges computed with different *k*. Note how the topology remains stable despite the overall increase in network density with increasing *k*. Frequency of edges appearance within the groups (*f*) is shown with color hues.

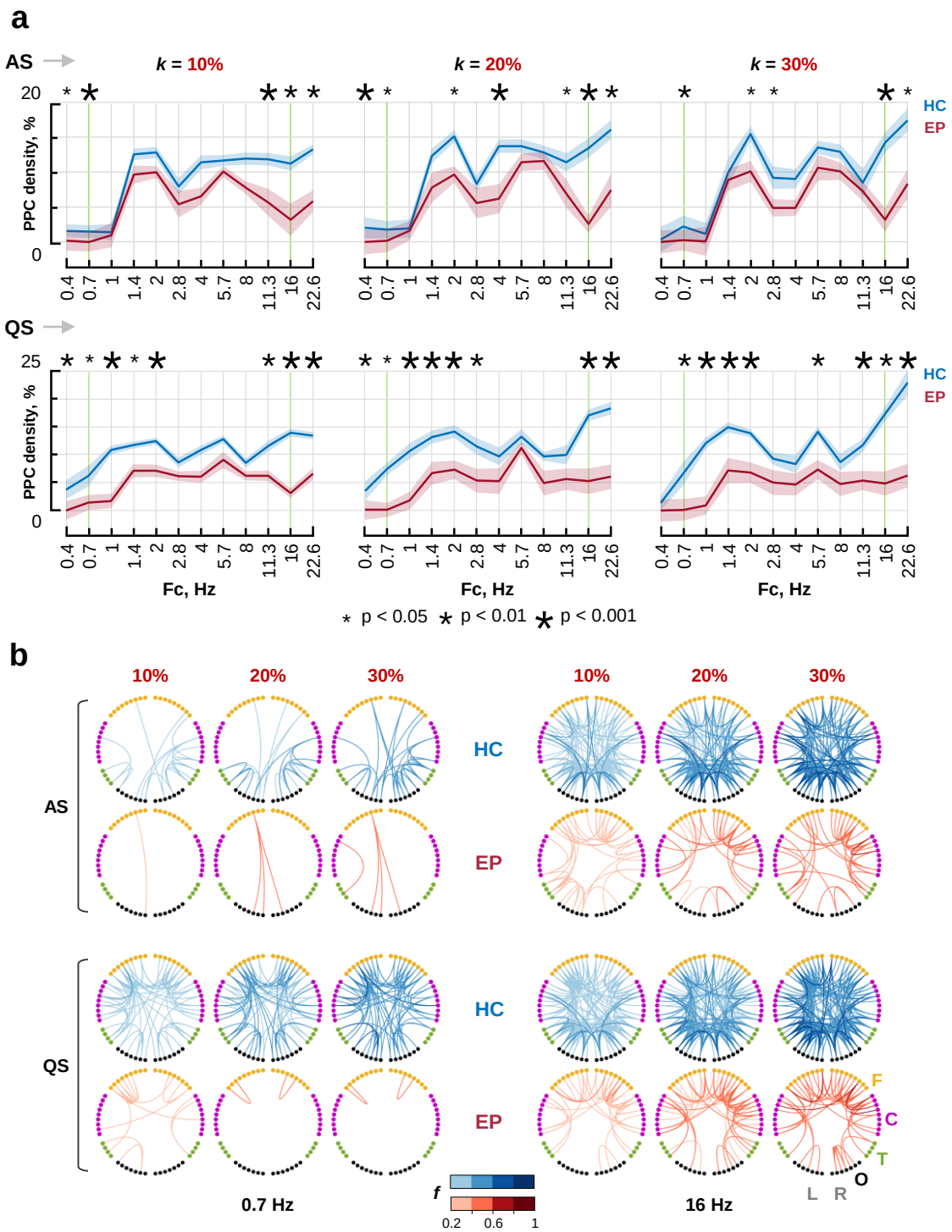

Figure S8. Effect of the threshold selection (*k*) on the consistent PPC networks and their comparison between Healthy Controls (HC) and Early Preterm (EP) infants. **a**, We reproduced the density comparisons (see **Methods** and **Supplemental** Fig. S5) using *k* = 10, 20, and 30%. The panels show results in active sleep (AS; top) and quiet sleep (QS; bottom). Statistical testing was performed using bootstrapping (*N* = 200 surrogates for each case). The results suggest that significant differences in densities between groups are robust to different *k* values. **b**, Examples of the spatial distributions of the consistent edges computed with different *k*. Note how the topology remains stable despite the overall increase in network density with increasing *k*. Frequency of edges appearance within the groups (*f*) is shown with color hues.

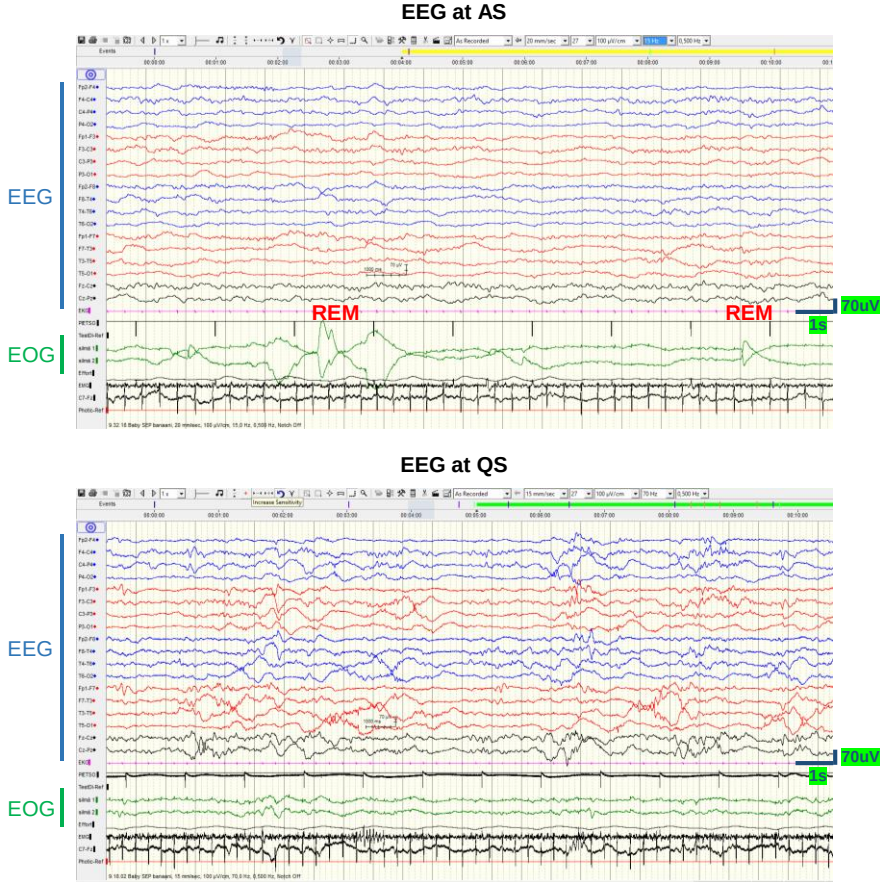

Figure S9. Exclusion of eye movement as a significant artefact. In theory, it could be reasoned that eye movements cause spurious connectivity between the frontal EEG electrodes. However, our observations from the neonatal EEG signals are not compatible with such idea. Perhaps the clearest evidence against contamination by eye movements is obtained by visual comparison of recordings during active sleep (AS) and quiet sleep (QS), which are known to associate with excessive eye movements (rapid eye movements; REM) and paucity of eye movements, respectively.

First, direct comparison of EEG and electrooculogram (EOG) during AS shows that there is very little if any EEG deflection related to eye movements. Second, these rapid eye movements give rise to low frequency (~1Hz) signals that could give rise to spurious phase-phase correlation (PPC) at the corresponding frequency, however AS has significantly less PPC at this frequency (see Figure 2a in the main article). Third, it would be hard to reconcile with eye movements the finding that amplitude-amplitude correlation (AAC) is so much stronger at wide range of frequencies.

Literature

Grossmann A, Kronland-Martinet R, Morlet J. 1989. Reading and understanding continuous wavelet transforms. In Wavelets, Springer, 2-20.

Korhonen O, Palva S, Palva JM. 2014. Sparse weightings for collapsing inverse solutions to cortical parcellations optimize M/EEG source reconstruction accuracy. J Neurosci Methods. 226:147-160.

Omidvarnia A, Fransson P, Metsäranta M, Vanhatalo S. 2014. Functional bimodality in the brain networks of preterm and term human newborns. Cereb Cortex. 24:2657-2668.

Palva JM, Monto S, Kulashekhar S, Palva S. 2010. Neuronal synchrony reveals working memory networks and predicts individual memory capacity. Proc Natl Acad Sci U S A. 107:7580-7585.